Theor Chem Acc (1999) 102:252–261
DOI 10.1007/s002149800m79

Theoretical
Chemistry Accounts

© Springer-Verlag 1999

Regular article

Generalization of coupled-cluster response theory to multireference expansion spaces: application of the coupled-cluster singles and doubles effective Hamiltonian*

Seiichiro Ten-no[1], **Suehiro Iwata**[1], **Sourav Pal**[2], **Debashis Mukherjee**[3]

[1] Institute for Molecular Science, Myodaiji, Okazaki 444-8585, Japan
[2] Theoretical Chemistry Group, Physical Chemistry Division, National Chemical Laboratory, Pune 411008, India
[3] Department of Physical Chemistry, Indian Association for the Cultivation of Science, Calcutta 700032, India

Received: 2 July 1998 / Accepted: 28 August 1998 / Published online: 11 November 1998

Abstract. Employing separate cluster ansatz in time-independent and time-dependent wave-operators, coupled-cluster (CC) response theory is generalized to multireference (MR) expansion spaces. For state energies, this corresponds to the MR secular problem with an arbitrary similarity-transformed effective Hamiltonian, $\tilde{H} = \Omega^{-1} H \Omega$. The effective Hamiltonian can be generated via size-extensive CC methods. Thus the states in MR linear response theory (MRLRT) maintain the usual CC core-extensive properties. We have used the Gelfand unitary group basis of the spin-adapted configurations to construct the matrix of $\tilde{H}$ in the MR excitation space. As a preliminary application, the CC singles and doubles effective Hamiltonian is applied to excitation and photoionization energies of the CH^+ and N_2 molecules, and is compared with experimental results and results from other numerical procedures including conventional CC linear response theory (CC-LRT), MR and full configuration interaction (MRCI and FCI) methods. The numerical results indicate that MRLRT reproduces valence and external excited states quantitatively, combining the best features of CC-LRT and MRCI.

Key words: Coupled-cluster theory – Response theory – Effective Hamiltonian – Multireference configuration space – Excited states – Core-extensive

1 Introduction

Single-reference coupled-cluster theory (SRCC) [1–2] has been well accepted as one of the most promising methods in ab initio molecular orbital theory, including infinite-order perturbational series in a size-extensive manner. Theoretical and algorithmic developments in CC theory enabled us to calculate static molecular properties accurately [3, 4] around the equilibrium geometry with a large one-electron expansion set [5]. For excited states and for bond dissociations, however, multireference (MR) model spaces are needed to reproduce quasi-degeneracy among states. The MRCC theories have been developed as Hilbert-space state-universal [6–8] and Fock-space valence-universal approaches [9, 10] in the complete and incomplete model spaces. Although these approaches are capable of treating excited and ionized states, it is difficult to avoid the intruder state problem which arises from the change of geometrical parameters. In this context, another important and growing field is the state-selective (SS) MRCC approaches [11–15] which are less sensitive to intruder states at any molecular geometry. As these methods are in principle for the lowest state in a given symmetry as in SRCC, additional methods are needed for energy differences.

Dynamic properties including excitation energies have been calculated from the CC responses. CC linear response theory (CC-LRT) based on the time-dependent CC formalism was first put forward by Monkhorst [16]. Many investigators later discussed in detail how to compute such dynamic properties [17–21]. For excitation energies, other CC-based terminologies have been used, such as the symmetry-adapted cluster configuration interaction (SAC-CI) method [22] and the equation of motion CC (EOM-CC) method [19, 23]. Besides approximations to the operator products and to the spin symmetry, all of these methods are essentially identical as long as energy differences are concerned. As the CC wave function is size-extensive, the CC-LRT features core-extensive properties in the excited-state wave function [24] and size-intensive excitation energies [21]. Recent important developments in this field are the atomic orbital (AO) integral driven approach [25] and the similarity-transformed EOM-CC method [26]. Especially, the latter makes it possible to ignore two-elec-

---

* Contribution to the Kenichi Fukui Memorial Issue

Correspondence to: S. Ten-no

tron excited determinants with the aid of notion in the Fock space approach.

It is well known that the excitation energies of the two- or more electron excited states are overestimated in the CC single and double LRT (CCSD-LRT) due to the lack of interactions between excited and remaining electrons. Thus MR model spaces are needed to calculate general excited states based on such SSCC methods. Some authors have investigated extensions of CC-LRT. SAC-CI employed the complete active space (CAS) and the exponentially generated CI spaces [27]. Recently, Ajitha and Pal [28] developed a time-dependent MRCC response approach. Another development of LRT from a different theoretical point of view has been suggested most recently by Chatterjee et al. [29], which is the linear response formulation of the state-specific MRCC method [14]. The present formulation is similar to that of Ajita and Pal and of Monkhorst [16], but features more flexible construction of the method employing individual wave-operators in time-dependent and time-independent components. Starting with such a time-dependent CC theory, we generalize CC-LRT to the MR expansion spaces (MRLRT) in Sect. 2. Spin-adapted configuration state functions (CSFs) based on the Gelfand unitary group, which have been used extensively in MRCI methods, are employed as expansion functions. A preliminary application of the CCSD effective Hamiltonian to MRLRT is investigated in Sect. 3. Results and discussions are given in Sect. 4.

2 Generalization of CC response theory

We start with a general response theory for a molecular system in the presence of an adiabatically switched-on perturbation,

$$\varsigma(t) = \sum_{\omega} \underline{\varsigma}(\omega) \mathrm{e}^{\alpha t - \mathrm{i}\omega t} \ , \tag{1}$$

where α is a real positive infinitesimal and $\underline{\varsigma}^{+}(\omega) = \underline{\varsigma}(-\omega)$ due to the hermitian nature of the Hamiltonian. Following the suggestion of Monkhorst [16], we use the time-dependent CC wave function in the exponential form,

$$\Psi(t) = \exp[R(t) - \mathrm{i}E_0 t]\Psi_0 \ , \tag{2}$$

where time-independent Ψ_0 and E_0 are the exact wave function and energy at $t = -\infty$, respectively, and the time-dependent vacuum phase factor, $\exp[-\mathrm{i}\varepsilon(t)]$, is implicitly put into the exponent, $R(t)$, which includes an imaginary identity operator. Most time-dependent CC theories assume that the time-independent and time-dependent amplitudes have the same structures of hole-particle excitations. We do not use this convention to make the present method more flexible. The time-dependent amplitudes are expanded by

$$R(t) = R^{(1)}(t) + R^{(2)}(t) + \cdots \ , \tag{3}$$

where the superscript indicates the order of expansion in ω as

$$R^{(1)}(t) = \sum_{\omega} \underline{R}^{(1)}(\omega + \mathrm{i}\alpha)\mathrm{e}^{\alpha t - \mathrm{i}\omega t} \ , \tag{4}$$

$$R^{(2)}(t) = \sum_{\omega_1 \omega_2} \underline{R}^{(2)}(\omega_1 + \mathrm{i}\alpha, \omega_2 + \mathrm{i}\alpha)\mathrm{e}^{2\alpha t - \mathrm{i}\omega_1 t - \mathrm{i}\omega_2 t} \ . \tag{5}$$

The wave function is transformed with an arbitrary time-independent wave-operator which does not change any physical property,

$$\Psi(t) = \Omega\tilde{\Psi}(t) \ . \tag{6}$$

Multiplying Ω^{-1} to the left, the time-dependent Schrodinger equation becomes,

$$\mathrm{i}\frac{d}{dt}\tilde{\Psi}(t) = [\tilde{H} + \tilde{\varsigma}(t)]\tilde{\Psi}(t) \ , \tag{7}$$

where the time-independent and time-dependent parts of the effective Hamiltonian are

$$\tilde{H} = \Omega^{-1} H \Omega \ , \tag{8}$$

$$\tilde{\varsigma}(t) = \Omega^{-1}\varsigma(t)\Omega \ . \tag{9}$$

We expand each order of the Fourier component associated with disconnected products of the exponential in terms of an orthonormalized basis function, $\{\Phi_\kappa\}$,

$$\begin{aligned} &\underline{R}(\omega_1 + \mathrm{i}\alpha, \ldots, \omega_2 + \mathrm{i}\alpha)\tilde{\Psi}_0 \\ &\quad = \sum_{\kappa} \Phi_\kappa \underline{r}_\kappa(\omega_1 + \mathrm{i}\alpha, \ldots, \omega_2 + \mathrm{i}\alpha) \ , \end{aligned} \tag{10}$$

including the time-independent part,

$$\tilde{\Psi}_0 = \sum_{\kappa} \Phi_\kappa c_{0\kappa} \ . \tag{11}$$

Equating contributions in power of ω and taking projections on Φ_κ yields an explicit expression of the time-dependent amplitudes. The first- and second-order equations convey information on the linear and the quadratic coefficients,

$$\underline{\mathbf{r}}^{(1)}(\omega) = -[\tilde{\mathbf{H}} - \omega\mathbf{I}]^{-1}\tilde{\underline{\boldsymbol{\varsigma}}}^{(1)}(\omega) \ , \tag{12}$$

$$\underline{\mathbf{r}}^{(2)}(\omega_1, \omega_2) = -[\tilde{\mathbf{H}} - (\omega_1 + \omega_2)\mathbf{I}]^{-1}\tilde{\underline{\boldsymbol{\varsigma}}}^{(2)}(\omega_1, \omega_2) \ , \tag{13}$$

where

$$(\tilde{\mathbf{H}})_{\kappa\lambda} = \langle \Phi_\kappa | \tilde{H} - E_0 | \Phi_\lambda \rangle \ , \tag{14}$$

$$(\tilde{\underline{\boldsymbol{\varsigma}}}^{(1)}(\omega))_\kappa = \langle \Phi_\kappa | \tilde{\underline{\varsigma}}(\omega) | \tilde{\Psi}_0 \rangle \ , \tag{15}$$

$$\begin{aligned} (\tilde{\underline{\boldsymbol{\varsigma}}}^{(2)}(\omega_1, \omega_2))_\kappa = \Big\langle \Phi_\kappa \Big| &\tilde{\underline{\varsigma}}(\omega_1) R^{(1)}(\omega_2) \\ &+ \tilde{\underline{\varsigma}}(\omega_2) R^{(1)}(\omega_1) \Big| \tilde{\Psi}_0 \Big\rangle \ . \end{aligned} \tag{16}$$

It is clear from the exponential structure of the wave function that all disconnected terms naturally vanish as a result of the lower-order expansion conditions as long as $\langle \Phi_\kappa | R(t)$ is a member of the expansion set. So the present form is identical to the usual expression using commutators. The straightforward calculation of expectation values of a time-independent operator requires evaluations of time-evolving density matrices, which include nonterminating series of operator products. Dalgaard and Monkhorst [18] discussed the connection between the vacuum amplitude in adiabatic perturbation theory and the level-shift function in CC theory for LR functions Koch and coworkers [21] proposed another method using biorthogonal counterparts of the ket states. We will discuss in detail the method calculating response functions elsewhere. The poles of the time-dependent coefficients correspond to the excitation energies including the initial state, $\omega = 0$, which are obtained by diagonalizing $\tilde{\mathbf{H}}$. In the present formulation, the choices of the wave-operator and the expansion set are arbitrary.

Variations in the choice of Ω, and the expansion space spanned by Φ_κ provide many possibilities of the method. Ideally, the former plays a role in reproducing universal properties as dynamic correlation effects, whereas the latter treats more or less state-specific properties such as near-degeneracy correlation, residual pair-collision and polarization effects. In CC-LRT, the wave-operator has an exponential form,

$$\Omega = \exp(T) \ . \tag{17}$$

Usually a subset of the expansion space induced by T is chosen as $\{\Phi_\kappa\}$. Accordingly the CC reference determinant is an eigenfunction in the absence of the perturbation, $\tilde{\Psi}_0 = \Phi_0$. In CCSD-LRT, $T = T_1 + T_2$, $\{\Phi_\kappa\}$ consists of the reference and the single and double substitutions. The orbital relaxation and the pair correlation effects are dealt with by the wave-operator and are put into the effective Hamiltonian. Thus CCSD-LRT reproduces any one-electron excited state including Rydberg series accurately around the equilibrium geometry (see Fig. 1a and b). The method, however, includes the following shortcomings. (1) Interactions between excited and remaining electrons are not included for two- or more electron excited states (Fig. 1c). Accordingly the excitation energies are overestimated for these states. (2) When the system stays away from the equilibrium atomic distances, the wave-operator starts to be dominated by near-degeneracy correlation effects, making the original LR expansion space insufficient. Apparently MR treatments are needed to overcome these difficulties and CSFs such as the Gelfand unitary group basis [30–34] can be employed. For state energies this corresponds to the MRCI secular problem in which H is replaced by $\tilde{H}$,

$$\langle \Phi_\kappa | \tilde{H} - (E_0 + \omega_I) | \tilde{\Psi}_I \rangle = 0 \ , \tag{18}$$

$$\tilde{\Psi}_I = \sum_{\kappa \in \mathrm{MRCI}} \Phi_\kappa c_{I\kappa} \ . \tag{19}$$

The ket eigenstates are nonorthogonal due to the nonhermiticity of $\tilde{H}$. One notes that the reference vacuum should be included in the expansion space in contrast to the usual CC-LRT, as the reference determinant is not necessarily the eigenfunction of $\tilde{H}$. To obtain an efficient wave-operator at any geometry, it is preferable to generate T amplitudes in MRCC methods. One possibility is to prepare all of the hole-particle excitation operators which induce the full MR expansion functions, borrowing the SR formalism,

$$T = T_1 + T_2 + \cdots + T_{N+M} \ , \tag{20}$$

$$T_k = \sum_{n_{\mathrm{ext}}=0}^{\min(N,k)} \sum_{n_{\mathrm{core}}=0}^{\min(N,k)} T_k^{(n_{\mathrm{ext}}, n_{\mathrm{core}})} \ , \tag{21}$$

where N and M are maximum excitation levels of the outer-valence and the valence excitations, and n_{ext} and n_{core} represent the external creation and the core annihilation levels, respectively. This kind of expansion has been investigated by Adamowicz and coworkers [13] in the SSMRCC method. Evaluations of T amplitudes and subsequent $\tilde{H}$, however, include tedious diagrammatic manipulations of nonlinear operator products. Furthermore, the state-selectivity in T away from the equilibrium geometry is not important as mentioned previously. Although it is possible to separate the state-specific portion, as a CAS wave function, $\exp(T^{\mathrm{val}})\Phi_0 \propto \Psi_{\mathrm{CAS}}$, the residual is still too complicated

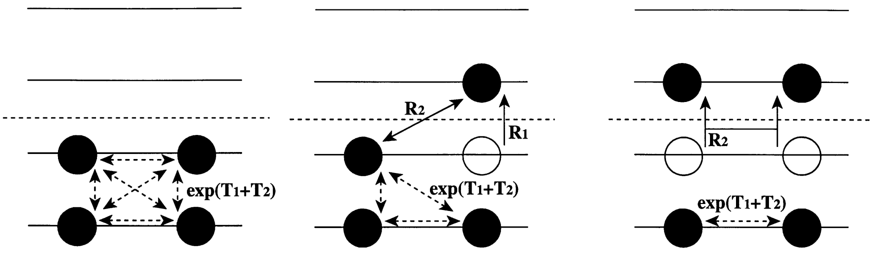

a) Closed Shell **b) 1E Excitation** **c) 2E excitation**

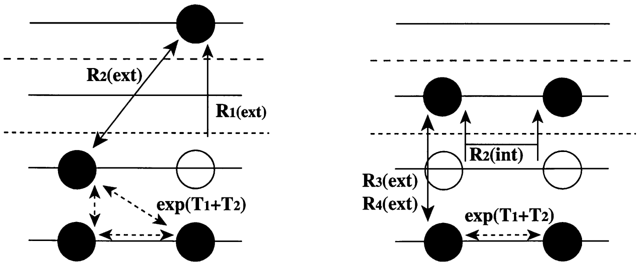

d) External 1E excitation **e) Valence 2E excitation**

Fig. 1a–e. Schematic representations of electronic states in coupled-cluster single and double linear response theory (CCSD-LRT) (**a–c**) and (MRLRT) with a CCSD effective Hamiltonian (**d, e**). The *black* and *white circles* represent occupied and vacant orbitals, respectively. The *arrows* denote interactions and excitations. Simultaneous interactions (*dotted arrows*) are included in the ground-state CCSD as $\exp(T_1 + T_2)$ (**a**), which ensures the core-extensivity of the CCSD-LRT wave functions (**b, c**). Pair interactions between excited and remaining electrons are not included for two-electron excited states in CCSD-LRT (**c**). In the MR picture, such states are treated as valence two-electron excited states (**e**) maintaining core-extensivity. Excitation levels of R are with respect to the closed shell vacuum to handle in large model spaces. In this particular work, we employ the CCSD effective Hamiltonian in MRLRT, which will be similar to that generated by operators in Eqs. (20) and (21) around the equilibrium geometry, focusing on general excited states. The valence and external Rydberg excited states are usually multi- and one-electron processes, respectively, as discussed in the SAC-CI method employing the exponentially generated CI space [27]. The present work emphasizes the use of MR expansion spaces in which efficient algorithms for matrix elements are readily available, treating one- and multi-electron processes in the external and valence spaces of the MR functions (Fig. 1d and e), respectively.

Before proceeding with an application of MRLRT, we summarize possible combinations with other methods for a wave-operator, Ω. The bond dissociation increases quasi-degeneracy among valence orbitals. To generate wave-operators which represent universal properties, it will be necessary to employ MRCC methods. One convenient form is the approximate MRCC wave-operator used by Banerjee and Simons [11]. Although the approximate form can treat only "external" excitations, the resulting $\tilde{H}$ has the same expression as the CCSD one. Furthermore, the ignored "internal" and "semi-internal" excitations can be treated afterward in MRLRT. In this way, first-order MRLRT will be a good approximation to describe any potential energy surface of valence excited states if the external correlation effects are transferable. For external excited states such as Rydberg series, external doubles are needed as the SR doubles in the usual CCSD-LRT. Treating these effects in terms of an exponential wave-operator leads to noncommutative algebra for cluster amplitudes such as $S(ei \rightarrow ee)$, where e and i represent external and internal lines, respectively. Use of the normal ordered exponential form, $\{e^S\}$, was proposed in the MRCC methods [6] and a similar idea was applied for excitation energies [26]. Such augmentations will be also possible in MRLRT.

3 Application of the CCSD effective Hamiltonian in MRLRT

Henceforward, $i, j, \ldots, a, b, \ldots$ and $p, q, \ldots$ denote the hole, particle and general labels of spatial orbitals, respectively. We assume that the reference function is a closed shell restricted Hartree-Fock (RHF) type determinant and that the T amplitudes are spin-adapted. Then, the CCSD effective Hamiltonian is spin-free and is conveniently written in terms of the unitary group generator, $E_{pr,qs,\ldots} = \sum_{\sigma\ldots\sigma'} a^+_{p\sigma} a^+_{q\sigma'} \ldots a_{s\sigma'} a_{r\sigma}$, by

$$\tilde{H} = \tilde{H}_0 + \tilde{H}_1 + \cdots + \tilde{H}_6 \ , \tag{22}$$

$$\tilde{H}_0 = \langle \Phi_0 | H \exp(T) | \Phi_0 \rangle \ , \tag{23}$$

$$\tilde{H}_1 = \sum_{pq} \langle p | \tilde{f} | q \rangle \{E_{pq}\} \ , \tag{24}$$

$$\tilde{H}_2 = \frac{1}{2} \sum_{pqrs} \langle pq | \tilde{V} | rs \rangle \{E_{pr,qs}\} \ , \tag{25}$$

and similar expressions for higher-body terms, where the braces represent normal ordering with respect to the RHF vacuum. The evaluation of $\tilde{H}$ is simplified by introducing a similarity-transformed Hamiltonian with $\exp(T_1)$, which does not change the operator rank of the original Hamiltonian,

$$\tilde{H} = \exp(-T_2) \hat{H} \exp(T_2) \ , \tag{26}$$

$$\begin{aligned} \hat{H} &= \exp(-T_1) H \exp(T_1) \\ &= \sum_{pq} \hat{h}_{pq} E_{pq} + \frac{1}{2} \sum_{pqrs} \langle pq | \hat{V} | rs \rangle E_{pr,qs} \ . \end{aligned} \tag{27}$$

This particularly useful transformation has been applied in AO integral-driven CC, CC-LRT [5, 25] and nonorthogonal CC methods [15]. Matrix elements of the effective Hamiltonian based on coupled-pair many electron theory or the CCD method were first derived by one of us up to two-body interactions [17]. In the present application, an expression identical to the similarity-transformed Hamiltonian, $\hat{H}$ can be used. Figure 2 shows Goldstone diagrams included in the CCSD effective Hamiltonian. The matrix elements, $\langle a | \tilde{f} | i \rangle$ and $\langle ab | \tilde{V} | ij \rangle$ are zero because of the CCSD condition. It is more convenient to express $\tilde{H}$ in the ordinary product form rather than the normal product one when evaluating matrix elements over CSFs. We can rewrite the effective Hamiltonian up to the two-body part in the ordinary product form,

$$\begin{aligned} \tilde{H} = &\sum_{pq} \langle p | \tilde{h} | q \rangle E_{pq} + \frac{1}{2} \sum_{pqrs} \langle pq | \tilde{V} | rs \rangle E_{pq,sr} \\ &+ \tilde{H}_3 + \cdots + \tilde{H}_6 \ , \end{aligned} \tag{28}$$

where we use the fact that $\tilde{H}_0$ does not affect the higher-body terms in the reverse hole-particle transformation. The matrix elements which are basic quantities in the present application are shown in Table 1.

Among the diagrams in $\tilde{H}_n$ ($n \geq 3$), single contractions which are linear to T_2, $T21a$ and $T21b$, are particularly important. In the usual CCSD-LRT, only a few shapes of the diagrams survive as discussed by Stanton and Bartlett [23b]. We assume that all of the hole indices belong to the internal orbital space in MRLRT but overlap between the particle and the valence orbital spaces is allowed, (see Fig. 3). In this case, all shapes of the diagrams should be considered due to the overlap. The present purpose is to devise a general MRLRT program utilizing state-of-the-art methods for coupling coefficients over CSFs. However, an efficient way to evaluate three-body coupling coefficients is not well known especially in the graphical unitary group approach [30–34], where one- and two-body coupling coefficients are generated efficiently by factorizations according to segment shapes. Furthermore, explicit treatment of the three-body matrix elements is costly.

▶

Fig. 2. Goldstone diagrams in the CCSD effective Hamiltonian. All T_1 operators are included implicitly in the energy vertices. *Horizontal arrows* denote both hole and particle indices

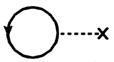
E10

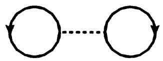
E20a

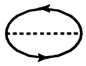
E20b

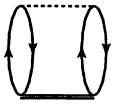
E21a

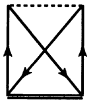
E21b

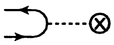
S10

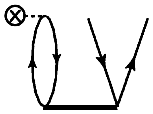
S11a

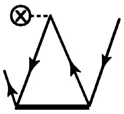
S11b

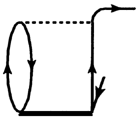
S21a

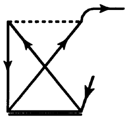
S21b

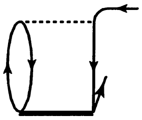
S21c

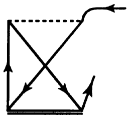
S21d

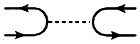
D20

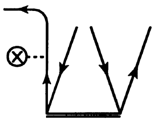
D11a

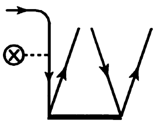
D11b

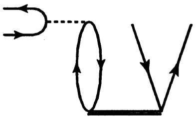
D21a1

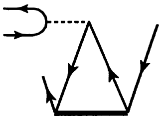
D21a2

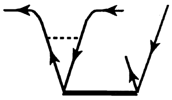
D21a3

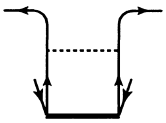
D21b

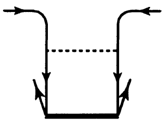
D21c

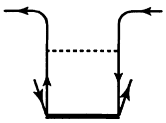
D21d

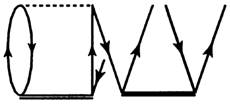
D22a

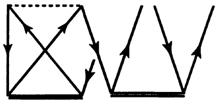
D22b

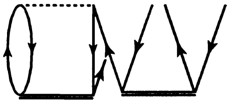
D22c

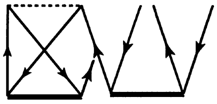
D22d

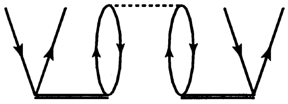
D22e

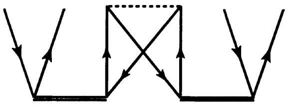
D22f

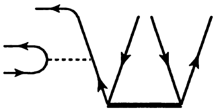
T21a

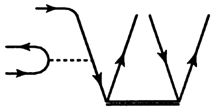
T21b

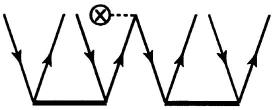
T12

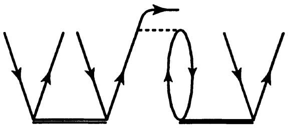
T22a

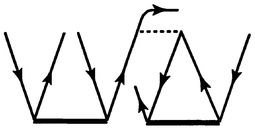
T22b

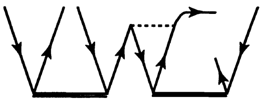
T22c

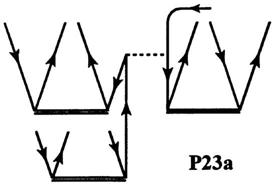
P23a

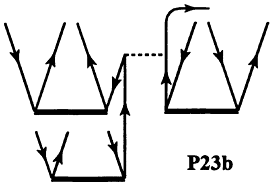
P23b

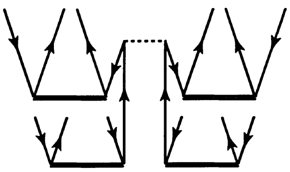
H24

Thus they should be treated "on-the-fly" during the iterative scheme which includes matrix-vector multiplication similar to that in the direct CI method,

$$\sigma_{I\kappa} = \sum_{\lambda} \langle \Phi_\kappa | \tilde{H} | \Phi_\lambda \rangle \mathrm{c}_{I\lambda} \ , \tag{29}$$

where $\boldsymbol{\sigma}_I$ is a residual of the trial vector $\mathbf{c}_I$. Another point is that inclusion of the three-body terms affects the entire part of the matrix element in the ordinary product form. In practice, it is simpler to apply the Wick theorem regarding the ordinary products as normal ordered ones, i.e. simply the creation operators are on the left of the annihilation ones. Some of the diagrammatic correspondences of the connected products in the ordinary product form are given in Table 2. It is always possible to decompose the three-body unitary group generators into one- and two-body ones. However, as each of the decomposed generators extends over the full spatial symmetry, this decomposition includes additional calculations of coupling coefficients, which are computationally less preferable. In this particular work, we include the three-body contributions in the reference space, $\lambda \in P$, which will dominate the weights in the MRLR expansion. In this case, r is a member of the internal orbitals. Introducing dummy orbitals, ζ, in each symmetry, using the relation,

$$E_{pr,q\zeta} E_{ai,\zeta j} = E_{pr,q\zeta,ai,\zeta j} + E_{ai,qj,pr} + \delta_{ra}(E_{pi,q\zeta,\zeta j} + E_{pi,qj}) \ , \tag{30}$$

and inserting the resolution of identity to the generator products, the three-body density part becomes

$$\boldsymbol{\sigma}^{\hat{V}Ts} = \boldsymbol{\sigma}^{\hat{V}Ts*} - \boldsymbol{\sigma}^{x'} \ , \tag{31}$$

$$\sigma^{\hat{V}Ts^*}_{I\kappa} = \sum_{\mu} \sum_{prqb} \langle \Phi_\kappa | E_{pr,q\zeta} | Y^{\zeta}_{\mu} \rangle \langle pq | \hat{V} | rb \rangle \mathrm{Q}^{(\mu)}_{I,b} \ , \tag{32}$$

$$\mathrm{Q}^{(\mu)}_{I,b} = \sum_{\mu\lambda} \sum_{abij} \langle ab | T_2 | ij \rangle \langle Y^{\zeta}_{\mu} | E_{ai,\zeta j} | \Phi_\lambda \rangle \mathrm{c}_{I\lambda} \ , \tag{33}$$

$$\sigma^{x'}_{I\kappa} = \frac{1}{2} \sum_{\lambda} \sum_{pqij} \langle pq | x' | ij \rangle \langle \Phi_\kappa | E_{pi,qj} | \Phi_\lambda \rangle \mathrm{c}_{I\lambda} \ , \tag{34}$$

$$\langle pq | x' | ij \rangle = \sum_{a \in \mathrm{internal}} \sum_{b} (1 + P_{ab}) \langle pq | \hat{V} | ab \rangle \langle ab | T_2 | ij \rangle \ , \tag{36}$$

where Y^{ζ}_{μ} denotes intermediate states which are first-order external CSFs to the dummy orbital, μ indicates occupations and spin-couplings of the $N-1$ electronic valence states and P_{ab} represents a permutation of the a and b orbital indices. We also use the fact that second-order intermediates can be excluded because of the valence orbital index, r. In a similar way, the residual of the $Ts\hat{V}$ part becomes

$$\boldsymbol{\sigma}^{Ts\hat{V}} = \boldsymbol{\sigma}^{Ts\hat{V}^*} + 2\boldsymbol{\sigma}^{y} \ , \tag{37}$$

$$\sigma^{Ts\hat{V}^*}_{I\kappa} = -\sum_{\mu} \sum_{abij} \langle \Phi_\kappa | E_{ai,b\zeta} | Y^{\zeta}_{\mu} \rangle \langle ab | T_2 | ij \rangle \mathrm{Q}^{(\mu)}_{I,j} \ , \tag{38}$$

Table 1. The effective Hamiltonian in the ordinary product form, including the energy, single- and double-open diagrams $(0+1+2)$[a]

Matrix element	Definition
$\langle a \vert \tilde{h} \vert i \rangle$	$\tilde{h}^a_i = -2\tilde{V}^{aj}_{ij} + \tilde{V}^{aj}_{ji}$
$\langle i \vert \tilde{h} \vert a \rangle$	$\tilde{h}^i_a = \hat{h}^i_a$
$\langle i \vert \tilde{h} \vert j \rangle$	$\tilde{h}^i_j = \hat{h}^i_j$
$\langle a \vert \tilde{h} \vert b \rangle$	$\tilde{h}^a_b = \hat{h}^a_b + (w^{ai}_{ib} - 2z^{ai}_{bi})/2$
$\langle ab \vert \tilde{V} \vert ij \rangle$	$\tilde{V}^{ab}_{ij} = 0$
$\langle ij \vert \tilde{V} \vert ak \rangle$	$\tilde{V}^{ij}_{ak} = \hat{V}^{ij}_{ak}$
$\langle ai \vert \tilde{V} \vert bc \rangle$	$\tilde{V}^{ai}_{bc} = \hat{V}^{ai}_{bc}$
$\langle ij \vert \tilde{V} \vert ab \rangle$	$\tilde{V}^{ij}_{ab} = \hat{V}^{ij}_{ab}$
$\langle ij \vert \tilde{V} \vert kl \rangle$	$\tilde{V}^{ij}_{kl} = (\hat{V} + x)^{ij}_{kl}$
$\langle ab \vert \tilde{V} \vert cd \rangle$	$\tilde{V}^{ab}_{cd} = (\hat{V} + y)^{ab}_{cd}$
$\langle ai \vert \tilde{V} \vert bj \rangle$	$\tilde{V}^{ai}_{bj} = (\hat{V} + z)^{ai}_{bj}$
$\langle ai \vert \tilde{V} \vert jb \rangle$	$\tilde{V}^{ai}_{jb} = (\hat{V} + w)^{ai}_{jb}$
$\langle ai \vert \tilde{V} \vert jk \rangle$	$\tilde{V}^{ai}_{jk} = (\hat{V} + u + w + x + z)^{ai}_{jk}$
$\langle ab \vert \tilde{V} \vert ic \rangle$	$\tilde{V}^{ab}_{ic} = (\hat{V} + v + w + y + z)^{ab}_{ic}$
$\langle ak \vert u \vert ij \rangle$	$u^{ak}_{ij} = u^{ka}_{ji} = \hat{f}^k_b t^{ab}_{ij}$
$\langle ab \vert u \vert ij \rangle$	$u^{ab}_{ij} = \hat{f}^b_c t^{ac}_{ij} + \hat{f}^a_c t^{cb}_{ij}$
$\langle ab \vert v \vert ic \rangle$	$v^{ab}_{ic} = v^{ba}_{ci} = -\hat{f}^j_c t^{ab}_{ij}$
$\langle ab \vert v \vert ij \rangle$	$v^{ab}_{ij} = -\hat{f}^k_j t^{ab}_{ik} - \hat{f}^k_i t^{ab}_{kj}$
$\langle pa \vert w \vert qi \rangle$	$w^{pa}_{qi} = w^{ap}_{iq} = \hat{V}^{pj}_{qb}(2t^{ab}_{ij} - t^{ab}_{ji}) - \hat{V}^{pj}_{bq} t^{ab}_{ij}$
$\langle ab \vert w \vert ij \rangle$	$w^{ab}_{ij} = \hat{V}^{ak}_{ic}(2t^{bc}_{jk} - t^{bc}_{kj}) - \hat{V}^{ak}_{ci} t^{bc}_{jk}$ $+ \hat{V}^{bk}_{jc}(2t^{ac}_{ik} - t^{ac}_{ki}) - \hat{V}^{bk}_{cj} t^{ac}_{ik}$
$\langle pq \vert x \vert ij \rangle$	$x^{pq}_{ij} = \hat{V}^{pq}_{ab} t^{ab}_{ij}$
$\langle ab \vert y \vert pq \rangle$	$y^{ab}_{pq} = \hat{V}^{ij}_{pq} t^{ab}_{ij}$
$\langle pa \vert z \vert iq \rangle$	$z^{pa}_{iq} = z^{ap}_{qi} = -\hat{V}^{pj}_{bq} t^{ab}_{ji}$
$\langle ab \vert z \vert ij \rangle$	$z^{ab}_{ij} = -\hat{V}^{bk}_{ci} t^{ac}_{kj} - \hat{V}^{ak}_{cj} t^{bc}_{ki}$

[a] Einstein summation convention is used

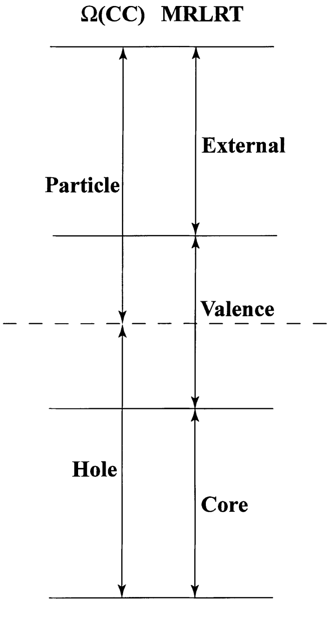

Fig. 3. Illustrative definitions of orbital spaces used in the CC and the MRLRT methods

Table 2. Diagrammatic correspondences of operators in $\hat{H}$ and $[\hat{H}, T_2]$

Symbol[a]	Operators	Diagrammatic correspondence	*W1*	*W2*[b]
$\hat{h}$	$\hat{h}^p_q E_{pq}$	*S10, E10*	*y*	*n*
$\hat{V}$	$\hat{V}^{pq}_{rs} E_{pr,qs}/2$	*D20, E20a, E20b*	*y*	*y*
$\hat{h}Ts$	$\hat{h}^p_b t^{ab}_{ij} E_{ai,pj}$	*D11a, S11a, S11b*	*y*	*y*
$Ts\hat{h}$	$-\hat{h}^j_b t^{ab}_{ij} E_{ai,bp}$	*D11b*	*n*	*y*
$\hat{V}Td$	$x^{pq}_{ij} E_{pi,qj}/2$	*D21b, S21a, S21b, E21a, E21b*	*y*	*y*
$Td\hat{V}$	$-y^{ab}_{pq} E_{ap,bq}/2$	*−D21c*	*n*	*y*
$\hat{V}Ts$	$\hat{V}^{pq}_{br} t^{ab}_{ij} E_{ai,pj,qr}$	*T21a, D21a, D21d, D11a, S21c, S21d, S11a, S11b*	*y*	*y*
$Ts\hat{V}$	$-\hat{V}^{pj}_{qr} t^{ab}_{ij} E_{ai,pq,br}$	*T21b, 2D21c, D11b*	*n*	*y*

[a] *Ts* and *Td* represent single and double contractions, respectively

[b] *W1* and *W2* represent diagrams included in the T_1 and T_2 working equations, respectively

$$\mathrm{Q}^{(\mu)}_{I,j} = \sum_{\mu\lambda} \sum_{pqrj} \langle jq|\hat{V}|pr\rangle \langle Y^{\zeta}_{\mu}|E_{\zeta p,qr}|\Phi_\lambda\rangle \mathrm{c}_{I\lambda} \ , \tag{39}$$

$$\sigma^{y}_{I\kappa} = \frac{1}{2} \sum_{\lambda} \sum_{abpq} \langle ab|y|pq\rangle \langle \Phi_\kappa|E_{ap,bq}|\Phi_\lambda\rangle \mathrm{c}_{I\lambda} \ . \tag{40}$$

The supplementary contributions, $\boldsymbol{\sigma}^{x'}$ and $2\boldsymbol{\sigma}^{y}$, are subtracted in the effective two-electron integrals prior to an iterative scheme. The matrix elements, $\langle a|\tilde{h}|i\rangle$ and $\langle ab|\tilde{V}|ij\rangle$, are determined such that the CCSD condition is satisfied. The resulting one- and two-body matrix elements are listed in Table 3. Both contributions of $\boldsymbol{\sigma}^{\hat{V}Ts}$ and $\boldsymbol{\sigma}^{Ts\hat{V}}$ are treated simultaneously by forming the vector $\mathrm{Q}^{(\mu)}_{I}$ whose size is equal to the number of orbitals in the symmetry of contracted lines for each μ. Although $\mathrm{Q}^{(\mu)}_{I}$ includes zero matrix elements, the computation time for these contributions is small. The effective Hamiltonian is diagonalized using a generalized Davidson procedure for non-hermite matrices [35–36], which gives a convergence similar to the usual CI secular problems.

4 Results and discussion

4.1 Excitation energies of CH^+

Full CI (FCI) results are available for the CH^+ molecule [37] which has been compared with results from Fock space MRCC, CCSD-LRT and analogous models [21, 23b, 38, 39]. The size of the system is small enough for calculations at any level. The previous results, however, show that it is difficult for CCSD-LRT to treat some low-lying states of this molecule which consists of two-electron excited configurations. It will be useful to employ the present MRLRT for such states. The $[5s3p1d/3s1p]$ basis set and the internuclear distance, $R = 2.13713$ a.u., are used as in Ref. [37]. We use natural orbitals based on the full valence state-averaged CASSCF calculation for the lowest two $^1\Sigma^+$ and one $^1\Delta$ states. The ground-state electronic configuration is $1\sigma^2 2\sigma^2 3\sigma^2$ with a relatively large double excitation, $T_2(3\sigma^2 \rightarrow 1\pi^2)$. We performed second-order MRLRT calculations with a reference space in which the four electrons are distributed in five orbitals, three σ and two π, and the $\sigma(1s)$ is treated as a core orbital, excitations of which are allowed by MRCI and the MRLRT. The three-body interactions linear to T_2 are included in the internal-internal (PP) block of the effective Hamiltonian matrix.

Table 3. The effective Hamiltonian in the ordinary product form, including the energy, single-, double- and linear triple-open diagrams $(0+1+2+3\mathrm{L})$[a]

Matrix element	Definition[b]
$\langle a\|\tilde{h}\|i\rangle$	$\tilde{h}^a_i = -2[\tilde{V} + u(2) + z/2]^{aj}_{ij} + [\tilde{V} + u(2) + W/2]^{aj}_{ji}$
$\langle i\|\tilde{h}\|a\rangle$	$\tilde{h}^i_a = \hat{h}^i_a$
$\langle i\|\tilde{h}\|j\rangle$	$\tilde{h}^i_j = \hat{h}^i_j$
$\langle a\|\tilde{h}\|b\rangle$	$\tilde{h}^a_b = \hat{h}^a_b$
$\langle ab\|\tilde{V}\|ij\rangle$	$\tilde{V}^{ab}_{ij} = -[u(2) + v(2) + w + x' + z]^{ab}_{ij}$
$\langle ij\|\tilde{V}\|ak\rangle$	$\tilde{V}^{ij}_{ak} = \hat{V}^{ij}_{ak}$
$\langle ai\|\tilde{V}\|bc\rangle$	$\tilde{V}^{ai}_{bc} = \hat{V}^{ai}_{bc}$
$\langle ij\|\tilde{V}\|ab\rangle$	$\tilde{V}^{ij}_{ab} = \hat{V}^{ij}_{ab}$
$\langle ij\|\tilde{V}\|kl\rangle$	$\tilde{V}^{ij}_{kl} = (\hat{V} + x - x')^{ij}_{kl}$
$\langle ab\|\tilde{V}\|cd\rangle$	$\tilde{V}^{ab}_{cd} = (\hat{V} + y)^{ab}_{cd}$
$\langle ai\|\tilde{V}\|bj\rangle$	$\tilde{V}^{ai}_{bj} = \hat{V}^{ai}_{bj}$
$\langle ai\|\tilde{V}\|jb\rangle$	$\tilde{V}^{ai}_{jb} = \hat{V}^{ai}_{jb}$
$\langle ai\|\tilde{V}\|jk\rangle$	$\tilde{V}^{ai}_{jk} = [\hat{V} + u(1) + x - x']^{ai}_{jk}$
$\langle ab\|\tilde{V}\|ic\rangle$	$\tilde{V}^{ab}_{ic} = [\hat{V} + v(1) + y]^{ab}_{ic}$

[a] The notation is same as in Table 1

[b] 1 and 2 in parentheses represent the one- and two-electron parts of $\hat{f}$ in u and v

In Table 4, we compare excitation energies. The MRCI results agree well with the FCI excitation energies for the valence excited states. The internal weight, however, decreases especially in $2^1\Sigma^+$ and $3^1\Sigma^+$, and accordingly the excitation energies are overestimated. On the other hand, for one-electron excited states, $2^1\Sigma^+$, $3^1\Sigma^+$, $1^1\Pi$ and $2^1\Pi$, the CCSD-LRT results are in good agreement with the FCI ones. The MRLRT results also agree even in the absence of the three-body interactions except for $3^1\Sigma^+$ which includes a non-negligible amount of two-electron excitations due to the CAS natural orbitals. The three-body interactions do not contribute to the energy matrix elements of the one-electron excited CSFs. Thus they are less important for one-electron processes. For the states $1^1\Sigma^+$, $1^1\Delta$ and $2^1\Delta$, the CCSD-LRT excitation energies are overestimated by 0.5–0.9

Table 4. Vertical excitation energies (eV) of the CH^+ molecule

State	Excitation[a]	FCI[b]	CCSD-LRT[c]	MRCI	MRLRT	
					0+1+2	0+1+2+3LPP
$^1\Sigma^+$	2	8.55	9.11	8.56	7.59	8.53
	1	13.52	13.58	13.85	13.43	13.51
	1	17.22	17.32	17.57	16.58	17.21
$^1\Pi$	1	3.23	3.26	3.23	3.24	3.20
	1	14.13	14.45	14.18	14.03	14.12
$^1\Delta$	2	6.96	7.89	6.97	6.68	6.93
	2	16.83	17.34	16.86	16.22	16.78
$^3\Pi$	1		1.03[d]	1.14	1.16	1.13
$\lvert\Delta E\rvert$		0.00	0.36	0.11	0.38	0.02

[a] Excitation levels of the main components of states based on the Hartree-Fock reference
[b] Ref. [37]
[c] Ref. [21b]
[d] Fock space MRCC result; Ref. [38]

eV. This is attributed to the lack of pair interactions between excited and remaining electrons. In MRLRT, these effects are treated; however, it is necessary to include the three-body diagrams which are as important as the residual dynamic correlation effects, 0.3–1.0 eV. MRLRT (0+1+2+3LPP) reproduces entire excitation energies accurately. This means that the best features of CCSD-LRT and MRCI are combined in MRLRT as described in Sect. 2.

4.2 Ionization energies of N2

Ionization processes of the N_2 molecule have been studied in terms of vacuum ultraviolet photoelectron spectra and compared with theoretical calculations [27, 40, 41]. As ionized states below about 30 eV are of valence character, the MRCI approach works well for these states. In this work, we use a relatively compact [$4s3p2d$] basis set of an augmented version of Dunning's correlation-consistent valence double zeta [42]. The d-type functions are used as six-component Gaussian-type functions. Natural orbitals are generated based on the full valence CASSCF in a way similar to the previous calculation with respect to the lowest $^1\Sigma_g^+$ and $^1\Delta_u$ states of N_2. The internuclear distance is assumed to be 2.035 a.u. In subsequent calculations of CCSD, MRCI and MRLRT, a couple of $1s$ orbitals are treated as frozen core. The lowest ionized states in the Σ_g^+, Π_u and Σ_u^+ symmetries are one-electron processes, i.e. simple detachments of single valence electrons. As the undetached electrons remain without orbital migrations, most of the dynamic correlation effects are included in the CCSD effective Hamiltonian. Thus it can be considered that such states can be treated by MRLRT with first-order external configurations to reproduce orbital relaxation effects, if the dynamic correlation is transferable between ionized and neutral states. We use a small CAS including only five doubly occupied valence orbitals of N_2, which is referred to as the S-model space. On the other hand, the other ionized states include excitations to π_g orbitals. To treat them, the two orbitals are added to the CAS, which is referred to as the L-model space. Although the linear three-body interactions are included as in the previous example, this makes no difference in the S-model space case.

Total and ionization energies from MRCI and MRLRT are shown in Table 5. In the S-model space calculation, the first-order results between the two methods are quite different. MRCI underestimates the ionization potentials by more than 2 eV due to the lack of treating dynamic correlation effects which are unbalanced between the neutral and ionized states. The large discrepancies are almost recovered at the second-order MRCI level. The differences between first- and second-order MRLRT are relatively small, 0.09–0.23 eV. The wrong direction at the second-order level is probably due to the size of the basis set and to the different definitions of the vertical ionization energies between theory and experiment. The first-order MRLRT model seems to be particularly useful considering the required computation time. It should be noted that we determined the wave-operator in a SS way with respect to the neutral state to maximize the discrepancy, which will be reduced by means of state-universal or less state-specific approaches for Ω.

The L-model space is sufficiently large for MRCI to reproduce the lowest seven ionized states. With this expansion space, the total MRLRT energies are slightly higher than the MRCI ones on average. This is probably due to the nonvariational nature of MRLRT and to the approximation of the three-body interactions used here. The differences in the excitation energies are, however, small and are within 0.1 eV. The experimental ionization energies are reproduced well both in MRCI and MRLRT. On the other hand, the $3\Sigma_g^+$ and $3\Sigma_u^+$ states include valence-Rydberg mixings. In MRCI, the choice of the active space is not sufficient to treat these states, whereas it is expected that MRLRT is capable of reproducing such mixings. Although there is a non-negligible discrepancy between MRLRT and experimental vertical ionization energies in the $3\Sigma_g^+$ state, recent extensive MRCI results [41] almost agree with our MRLRT ones for both $3\Sigma_g^+$ and $3\Sigma_u^+$.

Table 5. Ionization energies of N_2 from MRCI and MRLRT

State	MRCI			MRLRT			MRCI[c]	Expt[d]
	S/1st	S/2nd	L/2nd	S/1st	S/2nd	L/2nd		
$X^1\Sigma_g^{+}$[b]	−108.96134	−109.26198	−109.28846	−109.28539	−109.28539	−109.28605		
$X^2\Sigma_g^+$	13.54	15.70	15.40	15.50	15.41	15.33	(15.40)	15.58
$F^2\Sigma_g^+$			28.87			28.81	(28.87)	28.8
$3^3\Sigma_g^+$			–			33.10	(33.35)	31.01
$A^2\Pi_u$	14.65	16.67	16.80	17.08	16.97	16.76	–	16.93
$B^2\Sigma_u^+$	16.66	19.25	18.62	18.78	18.55	18.53	(18.67)	18.75
$C^2\Sigma_u^+$			25.31			25.30	(25.22)	25.51
$3^2\Sigma_u^+$			–			32.46	(32.64)	–
$1^2\Pi_g$			24.62			24.63	–	24.79
$D^2\Pi_g$			25.90			25.92	–	26

[a] Vertical ionization energies eV. S and L represent the small and the large CAS spaces, respectively. See the text

[b] Total energies of ground state N_2 in a.u

[c] An approximate value of the first vertical ionization energy, 15.40 eV, is added to the excitation energies of N_2^+ calculated by MRCI with ($7s6p2d1f$) Slater-type functions; Ref. [41]

[d] UV photoelectron spectroscopy; Ref. [40]

5 Conclusion

We generalized CC response theory to MR expansion spaces. In this method, arbitrary combinations of effective Hamiltonian and response expansion functions are possible, making use of individual structures in time-dependent and time-independent components of wave-operators. As a preliminary application, we calculated the excitation energies and ionization energies with the CCSD effective Hamiltonian. The numerical results for CH^+ showed that the best features of MRCI and CCSD-LRT are combined, maintaining core-extensivity as well as recovering defects of the methods, i.e. the lack of residual dynamic correlation effects in the multi-electron excited states in CCSD-LRT and difficulties of treating one-electron external excited states in MRCI. In the calculation of the one-electron ionization processes of N_2, transferability of the dynamic correlation effects is tested by comparing first- and second-order MRLRT. First-order MRLRT reproduced the experimental ionization energies well, making good use of the transferability. It is also demonstrated that all of the multi-electron valence ionization processes are treated accurately by second-order MRLRT.

To treat potential energy surfaces of general excited states with MRLRT, combinations with MRCC methods are necessary to generate wave-operators free from intruders. Some of these combinations are also discussed in this paper.

Acknowledgements. We would like to give a funeral address to Prof. Fukui in dedicating this paper. One of the authors (S.T.) acknowledges support by the Japanese Society for the Promotion of Science (JSPS) in Japan and the Department of Science and Technology (DST) in India. He is also thankful to Dr. D. Mukhopadhyay and Mr. K. Okada for useful discussions and to Mr. T. Tsurusawa for his technical assistance. The present work is partly supported by the Grant-in-Aids for Scientific Research (A) (No. 09304057) from the Ministry of Education, Science, Sports and Culture in Japan.

References

1. (a) Cizek J (1966) J Chem Phys 45:4151; (b) Cizek J, Paldus J (1971) Int J Quantum Chem 5:359
2. (a) Purvis GD, Bartlett RJ (1982) J Chem Phys 76:1910; (b) Bartlett RJ (1981) Annu Rev Phys Chem 32:359
3. (a) Salter EA, Tucks GW, Bartlett RJ (1989) J Chem Phys 90:1752; (b) Salter EA, Bartlett RJ (1989) J Chem Phys 90:1767
4. (a) Koch H, Jensen HJAa, Jørgensen P, Helgaker T, Scuseria GE, Schaefer HF III (1990) J Chem Phys 92:4924; (b) Kobayashi R, Koch H, Jørgensen P (1994) J Chem Phys 101:4956
5. (a) Koch H, Christiansen O, Kobayashi R, Jørgensen P, Helgaker T (1994) Chem Phys Lett 30:233; (b) Koch H, Sánchez de Merás A, Helgaker T, Christiansen O (1996) J Chem Phys 104:4157
6. (a) Lindgren I (1978) Int J Quantum Chem Symp 12:33; (b) Lindgren I, Mukherjee D (1987) Phys Rep 151:93
7. Jeziorski B, Monkhorst HJ (1981) Phys Rev A 24:1668
8. (a) Mukhopadhyay D Jr, Mukherjee D (1989) Chem Phys Lett 163:171; (b) Mukhopadhyay D Jr, Mukherjee D (1991) Chem Phys Lett 177:441; (c) Meissner L, Kucharski SA, Bartlett RJ (1989) J Chem Phys 91:6187; (d) Meissner L, Bartlett RJ (1990) J Chem Phys 92:561
9. (a) Mukherjee D, Moitra RK, Mukhopadhyay A (1975) Mol Phys 30:1961; (b) Mukherjee D, Moitra RK, Mukhopadhyay A (1977) Mol Phys 33:955; (c) Haque M, Mukherjee D (1984) J Chem Phys 80:5058
10. (a) Mukherjee D (1986) Chem Phys Lett 125:207; (b) Mukherjee D (1986) Int J Quantum Chem Symp 20:409
11. (a) Banerjee A, Simons J (1981) Int J Quantum Chem 14:207; (b) Banerjee A, Simons J (1982) J Chem Phys 76:4548
12. (a) Laidig WD, Bartlett RJ (1984) Chem Phys Lett 104:424; (b) Laidig WD, Saxe P, Bartlett RJ (1987) J Chem Phys 86:887; (c) Tanaka K, Terashima H (1984) Chem Phys Lett 106:558
13. (a) Oliphant N, Adamowicz L (1991) J Chem Phys 94:1229; (b) Oliphant N, Adamowicz L (1992) J Chem Phys 96:3739; (c) Adamowicz L, Malrieu J-P (1996) J Chem Phys 105:9240
14. (a) Mahapatra US, Datta B, Bandyopadhyay B, Mukherjee D (1998) Adv Quantum Chem 30:163; (b) Mahapatra US, Datta B, Mukherjee D (1998) Mol Phys 194:157
15. Ten-no S (1997) Theor Chem Acc 98:182
16. Monkhorst HJ (1977) Int J Quantum Chem Symp 11:421
17. (a) Mukherjee D, Mukherjee PK (1979) Chem Phys 39:325; (b) Datta B, Sen P, Mukherjee D (1995) J Phys Chem 99:6441

18. Dalgaard E, Monkhorst HJ (1983) Phys Rev A 28:1217
19. Sekino H, Bartlett RJ (1984) Int J Quantum Chem 18:255
20. (a) Arponen JS, Bishop RF, Pajanne E (1987) Phys Rev A 36:2519; (b) Arponen JS, Bishop RF, Pajanne E (1987) Phys Rev A 36:2537
21. (a) Koch H, Jørgensen P (1990) J Chem Phys 93:3333; (b) Koch H, Jensen HJAa, Jørgensen P, Helgaker T (1990) J Chem Phys 93:3345
22. Nakatsuji H (1978) Chem Phys Lett 39:562
23. (a) Geertsen J, Rittby M, Bartlett RJ (1989) Chem Phys Lett 164:57; (b) Stanton JF, Bartlett RJ (1993) J Chem Phys 98:7029
24. (a) Mukhopadhyay D, Mukhopadhyay S, Chaudhuri R, Mukherjee D (1991) Theor Chim Acta 80:441; (b) Mukherjee D, Pal S (1989) Adv Quantum Chem 20:291
25. Christiansen O, Koch H, Halkier A, Jørgensen P, Helgaker T, Sánchez de Merás A (1996) J Chem Phys 105:6921
26. Nooijen M, Bartlett RJ (1997) J Chem Phys 106:6441
27. (a) Nakatsuji H (1985) J Chem Phys 83:713; (b) Ehara M, Nakatsuji H (1998) Chem Phys Lett 282:347
28. Ajitha D, Pal S (1998) Phys Rev A 56:2658
29. Chatterjee S, Mahapatra US, Mukherjee D (1998) In: Hirao K (ed) Recent developments in multi-reference methods. World Scientific, Singapore, (in press)
30. (a) Paldus J (1974) J Chem Phys 61:5321; (b) Paldus J, Boyle MJ (1980) Phys Scr 21:295
31. (a) Shavitt I (1977) Int J Quantum Chem 11S:131; (b) Shavitt (1978) I Int J Quantum Chem 12S:5
32. Siegbahn PE (1980) J Chem Phys 72:1647
33. Pauncz R (1995) The symmetric group in quantum chemistry. CRC Press, Boca Raton
34. J. Hinze (ed) (1981) The Unitary group for the evaluation of electronic energy matrix elements. Springer, Berlin Heidelberg New York
35. Davidson ER (1975) J Comput Phys 17:87
36. Hirao K, Nakatsuji H (1982) J Comput Phys 45:246
37. Olsen J, Sánchez de Merás M, Jensen HJAa, Jørgensen P (1989) Chem Phys Lett 154:380
38. Vaval N, Pal S, Mukherjee D (1998) Theor Chem Acc 99:100
39. Rico RJ, Lee TJ, Head-Gordon M (1994) Chem Phys Lett 218:139
40. Baltzer P, Larsson M, Karlsson, Wannberg B, Göthe MC (1992) Phys Rev A 46:5545
41. Honjou N, Miyoshi E (1998) J Mol Struct (Theochem) (in press)
42. Dunning TH Jr (1988) J Chem Phys 90:1007